Design of a direct connection scheme of supercapacitors to the grid-tied photovoltaic system

Yoga Sandi Perdana, S. M. Muyeen*, Ahmed Al-Durra**

**Electrical Engineering Department, The Petroleum Institute, Abu Dhabi, United Arab Emirates*

Keywords: photovoltaic (PV) system, grid-tied, direct connection, supercapacitors, MPPT.

Abstract

A maximum power-point tracking (MPPT) technique needs to be applied to the photovoltaic (PV) system in order to extract maximum possible power output under those varying conditions. The development of supercapacitor (SC) as high power storage device in recent years has created opportunity to replace electrolytic capacitor by SC as dc-link capacitor to provide power during fault ride-through (FRT) condition. However, due to its much bigger capacitance, the voltage dynamics of SC is much slower compared to electrolytic capacitor. Therefore, in this paper, a MPPT technique using a string of supercapacitors which is directly connected to the DC-link of a PV generation system is proposed. The direct connection is proposed to avoid one stage DC-DC power conversion to implement MPPT, so that the efficiency of the system is increased. The proposed direct connection of supercapacitors string configuration along with MPPT strategy is verified by simulation analysis using MATLAB/Simulink where real solar irradiance data is used.

1 Introduction

The device used to convert the solar radiation into electricity is photovoltaic (PV) cell. Due to policies from governments around the world to reduce greenhouse effect caused by the burning of fossil fuels, the portion of power generated from grid-connected PV system has been increasing rapidly. It is reported that total installed capacity of PV power generation is increased more than 8 times in the period between 2009 and 2014 (from 20.4 GW to 177 GW) [1]. This represents about 1% of the world's electricity generation. Moreover, with the constantly reducing production cost of PV module, the return of investment of PV system installation is shorter [2]. Another advantage of grid-connected PV system is that it does not require storage devices and charge regulator since the grid acts as an infinite storage system. This can reduce the cost of grid-connected PV system about 40% less than the cost of stand-alone PV system [3]. Hence, people are encouraged to install the grid-tied PV generation system.

The distributed energy coming from the solar radiation is available in abundant amount. However, the power generated from a PV system is greatly influenced by the atmospheric conditions, mainly irradiance and temperature. Therefore, a maximum power point tracking (MPPT) algorithm is required to extract maximum possible power from PV panel under those varying irradiance and temperature conditions. Various power converter topologies, characterized by two-stage or single-stage, with transformer or transformerless, and with two-level or multilevel inverter, have been employed to transmit the power generated from the PV systems into the utility grid [4]. Typically, a PV string is interconnected to the grid through grid-tied solar inverter as shown in Figure 1 above. What commercially named "grid-tied solar inverter" is actually consisted of a dc-dc converter (usually Boost) as MPPT and a dc-ac inverter to control real/reactive power flow to the grid. As there are two conversion stages, dc-dc and dc-ac, the structure is named dual stage inverter.

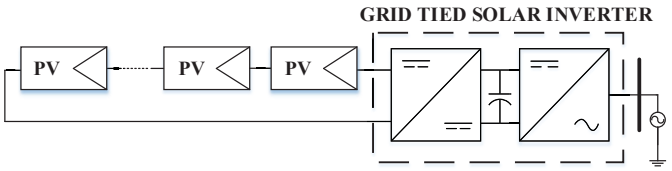

Figure 1: Dual stage inverter PV system

The grid-tied inverter is used to maintain constant DC voltage by controlling the voltage of the electrolytic capacitor. During short-term fault ride-through (FRT) condition, the power is stored the capacitor. This power imbalance makes the DC-link voltage increase and might cause a trip in the inverter. The larger the capacitance, the better its capability to handle dc voltage variation and power excursion in the dc-link [5]. However, the larger the capacitance is, the slower the dynamics of the dc voltage.

The applications of supercapacitor (SC) has been growing in recent years because of the development of materials and manufacturing process which lowered the production cost of SC. Due to its high-power characteristics, it is used to smooth a fast change in PV power output [6]. Compared to electrolytic capacitor whose capacitance is in order of microfarad, SC has much larger capacitance in order of farads and can store higher energy. The SC also has a longer cycle life which is around 1 million cycles. Another advantage of SC is that it does not require an overcharging protection circuit since it will not draw more current once it is fully charged [7]. However, due to its high capacitance, its voltage dynamics is slower than the electrolytic capacitor.

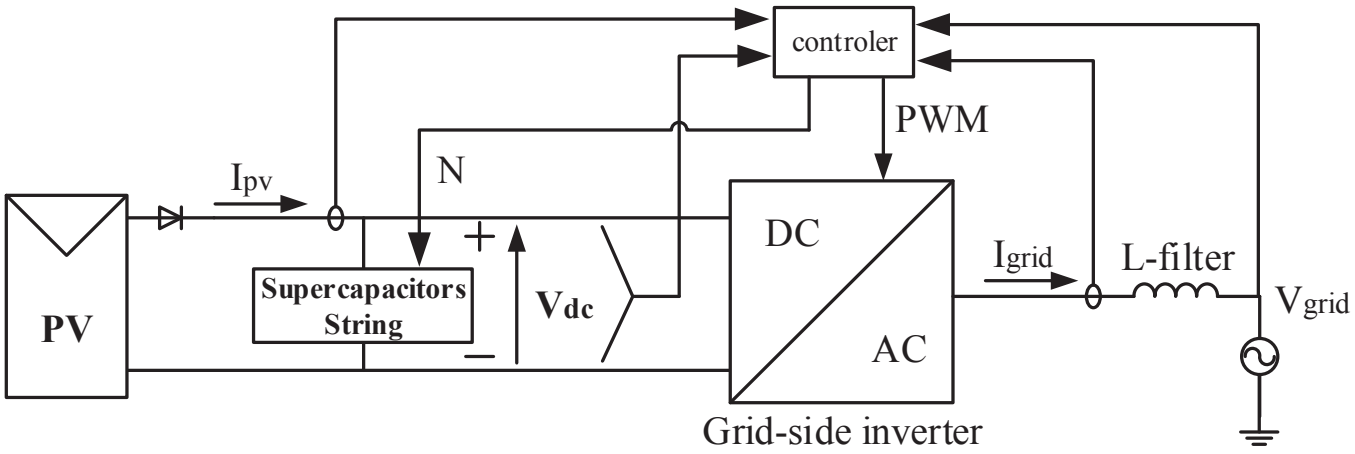

Figure 2: Proposed direct connection of supercapacitors string scheme

In [8], a direct connection of SCs into the PV terminal is presented. The SCs are used to compensate the fast change in PV output to control the ramp-rate of the power transmitted to the grid. The MPPT is not considered in that study since it will complicate the ramp-rate strategy. A combination of hydro-pneumatic storage and directly connected SCs into the PV terminal are discussed in [9]. The SCs are used to perform the proposed on-off MPPT which improves the system global efficiency. However the efficiency of proposed MPPT technique still has to be optimized compared to the conventional MPPT.

Therefore, in this study, a direct connection of a supercapacitors string as shown in Figure 2 is proposed to apply the MPPT. The SCs string is composed of several SC unit connected in series. As mentioned before, SC has a slow voltage dynamics. Hence, the basic idea to vary the voltage of the proposed configuration is by connecting or disconnecting the SC units. The detailed MPPT strategy of the proposed scheme is explained later in separate section. The effectiveness of the proposed configuration is validated using MATLAB/Simulink with realistic irradiation dataset.

2 Modelling of the proposed topology

A PV module consists of a number of PV cells which are semiconductor materials similar to PN junction diode to directly convert sunlight (photons) into electricity (electron charges) or electric current. Several PV modules can be connected in series to make a PV string. Several PV strings can be combined in parallel to create a PV array.

2.1 Modelling of PV module

Practical model of a single PV module is shown in Figure 3 [10]. In reality, PV modules are combined in series or parallel to obtain a certain voltage and power. Hence, aggregated model is used in simulation as explained in [11]. The output current and voltage of the aggregated model is expressed by

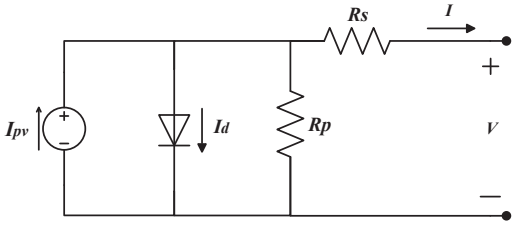

Figure 3: Practical model of a PV module

$$I = N_p I_{pv} - N_p I_0 \left[\exp\left(\frac{q\left(V + \frac{N_s R_s}{N_p} I \right)}{N_c N_s kTa} \right) - 1 \right] - \frac{V + \frac{N_s R_s}{N_p} I}{\frac{N_s R_p}{N_p}} \quad (1)$$

where I_{pv} and I_0 are the photo-current and reverse saturation current of the PV module respectively. N_s is the number of modules in a string and N_p is the number of strings connected in parallel.

2.2 Modelling and control of grid-side inverter

Three-phase inverter with L-filter model as depicted in Figure 4 is chosen as the model of the grid-side inverter of the proposed topology of PV system under study. The grid-side of the three-phase inverter is regulated by the following equations [12]:

$$\begin{aligned} \frac{di_a}{dt} &= -\frac{R}{L} i_a - \frac{1}{L} e_a + \frac{v_{dc}}{L} S_a \\ \frac{di_b}{dt} &= -\frac{R}{L} i_b - \frac{1}{L} e_b + \frac{v_{dc}}{L} S_b \\ \frac{di_c}{dt} &= -\frac{R}{L} i_c - \frac{1}{L} e_c + \frac{v_{dc}}{L} S_c \end{aligned} \quad (2)$$

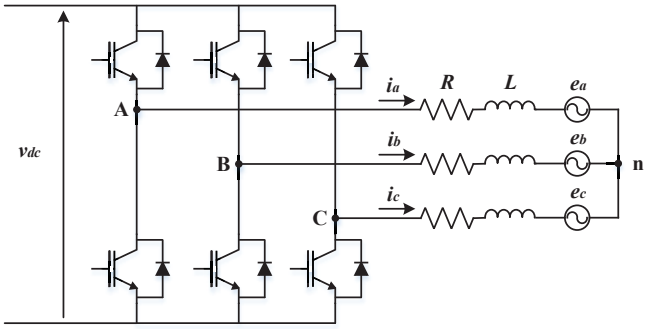

Figure 4: Grid-connected inverter with L-filter

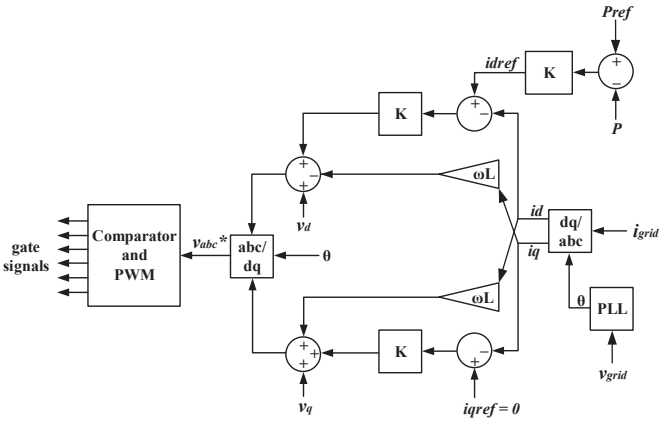

Figure 5: Grid connected inverter control diagram

where S_a, S_b, and S_c are the inverter switching signal input. By applying Park's transformation, time-invariant model in the dq frame rotating at grid angular frequency ω can be obtained as

$$\frac{di_d}{dt} - \omega i_q = \frac{1}{L}\left[-Ri_d - e_d + S_d v_{dc}\right]$$
$$\frac{di_q}{dt} + \omega i_d = \frac{1}{L}\left[-Ri_q - e_q + S_q v_{dc}\right] \qquad (3)$$

where S_d and S_q are the switching signal input and i_d and i_q are the output. By using a phase-locked loop (PLL) [13] to estimate angular position θ such that e_q is equal to zero and assuming the system is working in unity power factor, from the instantaneous power theory, the reference for the three-phase inverter controller can be calculated as

$$I_{dref} = \frac{2}{3}\frac{P_{ref}}{E_d}$$
$$I_{qref} = 0 \qquad (4)$$

where E_d is the maximum value of phase voltage of the grid. Therefore, the active power transmitted to the grid can be controlled by giving the reference P_{ref} to the inverter. Control diagram of the grid-connected inverter is shown in Figure 5. This control structure is based on the synchronous reference frame control with cross-coupling terms and voltage feedforward mentioned in [14].

2.3 Modelling and control of supercapacitor string

A simple resistive capacitive (RC) circuit is not adequate to represent a SC. A distributed model consists of three RC branches is presented in [15] to characterize the terminal behaviour of a SC. The distributed model of SC is shown in Figure 6. The parameters are based on the datasheet of BCAP0350 from Maxwell Technologies [16]. The parameters used in the simulation are presented in Table 1.

Capacitance (F)		*Internal Resistance (mΩ)*	
C_{b1}	7	R_{b1}	0.128
C_{b2}	175	R_{b2}	3.2
C_{b3}	168	R_{b3}	3.072

Table 1: The distributed parameters of the SC.

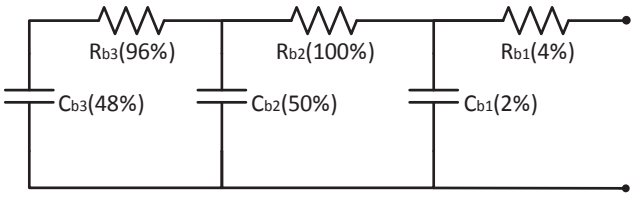

Figure 6: Distributed model of SC

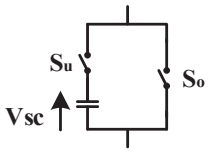

Figure 7: One single SC unit

The supercapacitors string shown in Figure 2 is arranged from several SC units connected in series. This SC unit is illustrated in Figure 7. A single SC unit consists of one SC with maximum voltage 2.7 V and two switches, S_u and S_o. Both the switches work in opposite way which mean when one switch is closed, the other is open, and vice versa. Therefore, the voltage of the unit is either equal to SC voltage or zero.

3 MPPT strategy

The proposed MPPT strategy is to match the number of connected SC units according to the maximum power operating voltage. The maximum power operating voltage can be obtained using any conventional MPPT method. Fractional open circuit voltage method is used in this study due to its simplicity.

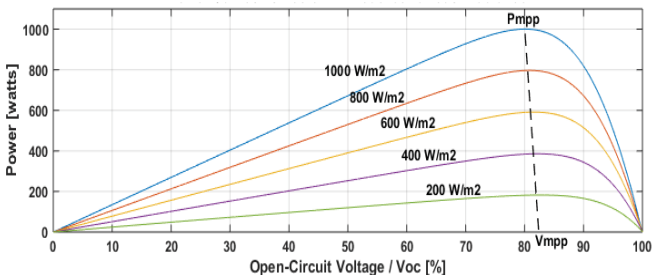

Figure 8: Power vs open-circuit voltage of the PV modules

3.1 Fractional open-circuit voltage

The value of I_{pv} in equation (1) is influenced by solar irradiance and temperature. MPPT technique is applied to match the operating voltage or current such that gives the maximum power output for a certain irradiance and temperature can be extracted [17]. There are many kind of MPPT techniques, some of them are Hill Climbing/P&O, Incremental Conductance, Fractional Open-Circuit Voltage, and Fractional Short-Circuit Current. Fractional Open-Circuit Voltage (FOCV) is used in this study due to its simplicity though other MPPT techniques can also be applied.

The FOCV technique is derived from the closely linear relation characteristic of PV maximum power point, V_{MPP}, and open circuit voltage, V_{OC}, for various irradiances as illustrated in Figure 8. Hence, V_{MPP} can be approximated as a fraction of V_{OC}.

$$V_{MPP} \approx k_{MPP} \times V_{OC} \tag{5}$$

where k_{MPP} is a constant which is approximated as 0.8 of V_{OC} for the PV module used in this study. In order to avoid temporary loss of power when PV modules are disconnected to measure the V_{OC}, a pilot cell is optimally chosen from PV module to obtain the V_{OC} which gives maximum power output without disconnecting the PV modules.

3.2 Supercapacitor string control strategy

In the proposed scheme, the MPPT is carried out by the SC string. The DC voltage varies by connecting or disconnecting the SC units in the string. The number of the connected SC units is determined according to the V_{MPP} reference obtained from FOCV method in equation (5). Hence, the number of the connected SCs is then a function of V_{MPP} and the supercapacitor unit voltage, V_{SC} as follows.

$$N = f\left(V_{MPP}, V_{SC}\right) = \begin{cases} N_{prev} - 1, \mathrm{mod}\left(V_{MPP}, V_{SC}\right) < V_{SC}/2 \\ N_{prev} + 1, \mathrm{mod}\left(V_{MPP}, V_{SC}\right) \geq V_{SC}/2 \end{cases} \tag{6}$$

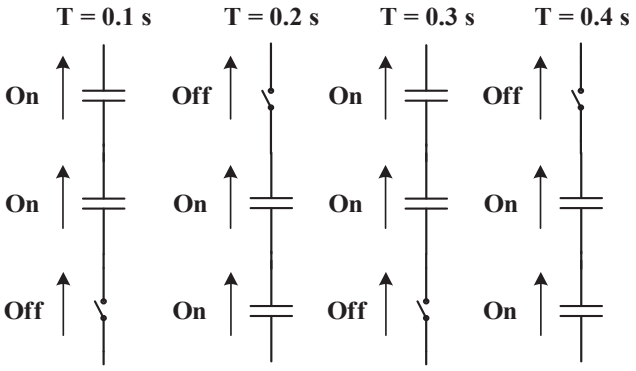

Figure 9: Time-shifting method illustration

where N is the number of connected SCs, N_{prev} is the previous number of connected SC, and mod is modulo operation.

3.3 Switching load balancing

In order to maintain the balance of the switching loading and state of charge (SOC) of each SC units, a Time-Shifting algorithm [18] is employed. A shifting time period of T = 0.1 second is adequate as the change in solar irradiance is not as fast as wind speed. This method means that the SC connections are shifted every 0.1 s while keeping the number of connected SCs constant. A simplified illustration with 3 SC units and N is set to 2 is shown in Figure 9.

3.4 Supercapacitor switching reduction

The rapid changes in irradiance, i.e. due to moving clouds, might create very fast changes in the V_{MPP} reference which can ruin the time-shifting algorithm and the load balancing method. Therefore, an On/Off delay block in Simulink is placed in the determination of connected SCs number, N. The function of the delay block is to hold the reference value constant unless it changes after specified time [19].

4 Cost analysis

In order to check the economic feasibility of the proposed configuration, its production cost is compared with the conventional topology shown in Figure 1. Study cases of 6 kWp and 250 kWp grid-tied PV system are taken for residential and commercial scale respectively. The results are shown in Table 2 and Table 3.

As can be seen, even though cost of the proposed scheme is higher for residential scale case, it is the opposite for commercial scale. Hence, it might be commercially feasible to implement the proposed topology for a commercial scale grid-tied PV generation system. However, the results of the cost comparison could be different if the maintenance and replacement of components cost are taken into consideration since SC has longer cycle life than electrolytic capacitor.

Residential scale			
Conventional topology			
Component	Unit price ($)	Unit	Price ($)
DC inductor filter	30.57	20	611.4
Switches	48.62	1	48.62
Switch drivers	86.92	1	86.92
Heat sinks	38.27	1	38.27
Cooler fan	133.93	1	133.93
DC-link capacitor	61.86	1	61.86
Total			981.00
Proposed topology			
Component	Unit price ($)	Unit	Price ($)
Switches	48.62	36	1750.32
Switch drivers	86.92	36	3129.12
Supercapacitors	11.81	396	4676.76
Total			9,556.20

Table 2: Cost comparison for residential scale case

Commercial scale			
Conventional topology			
Component	Unit price ($)	Unit	Price ($)
DC inductor filter	30.57	720	22010.4
Switches	203.38	1	203.38
Switch drivers	113.45	1	113.45
Heat sinks	38.27	1	38.27
Cooler fan	133.93	1	133.93
DC-link capacitor	194.11	4	776.44
Total			23,275.87
Proposed topology			
Component	Unit price ($)	Unit	Price ($)
Switches	203.38	36	7321.68
Switch drivers	113.45	36	4084.2
Supercapacitors	11.81	792	9353.52
Total			20,759.40

Table 3: Cost comparison for commercial scale case

5 Simulation results

The validity of the proposed configuration and the MPPT strategy has been checked using MATLAB/Simulink. In this paper, the model of the PV module is based on Kyocera KC200GT solar module whose parameters can be found in [10]. The parameters of the system used in the simulations are listed in Table 4. Real PV output data taken in The Petroleum Institute, Abu Dhabi, UAE, on October 10, 2008 which is shown in Figure 10 is used to verify the effectiveness of the system. The DC voltage varies from 120 to 132 V.

The dc-link voltage and its reference are shown in Figure 11. As can be seen, the dc voltage follows the reference MPP voltage. The voltage varies in a step fashion since it is performed by connecting/disconnecting the SC units. However, the MPPT is not applied when the reference is below the battery voltage due to limitation in the DC-link voltage variations. The MPPT effectiveness can be improved by using smaller voltage step change.

Maximum power of PV panel (Wp)	1000
Supercapacitor unit voltage (V)	2
Line-to-line grid voltage (V)	66
Inverter inductance (mH)	12
Frequency (Hz)	50

Table 4: Simulation parameters

The power transmitted to the grid are shown in Figure 12. It can be seen that the active power transmitted to the grid is the maximum power obtained from the proposed MPPT method. It follows the power reference given to the inverter.

Figure 13 shows the current output of the grid-side inverter. From its shape, it can clearly be known that the THD of the current is low despite the variation in dc-link voltage. Hence, the MPPT strategies are valid.

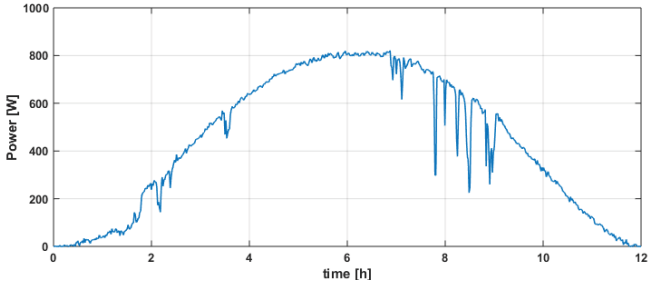

Figure 10: PV generation data

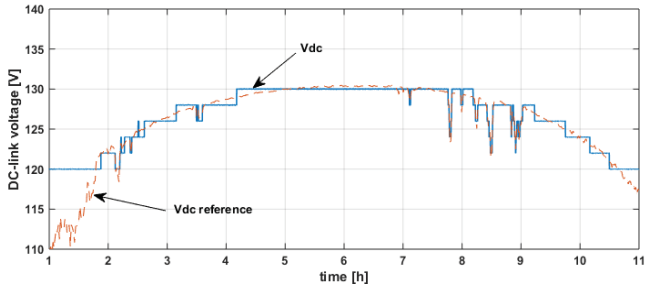

Figure 11: DC-link voltage

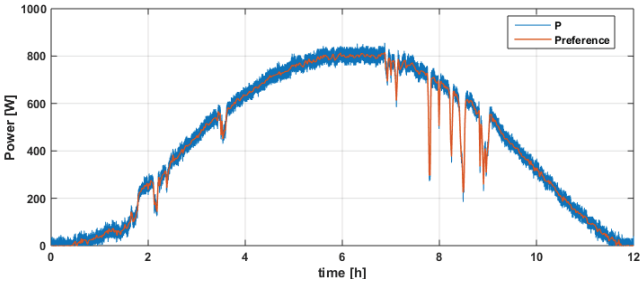

Figure 12: Power transmitter to the grid

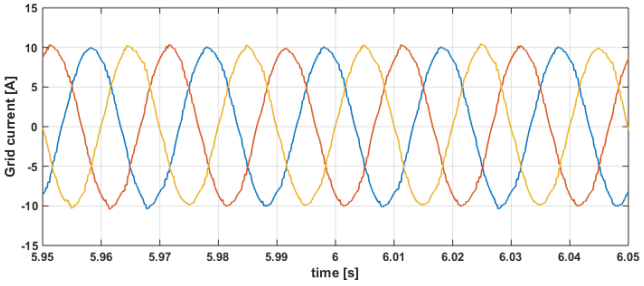

Figure 13: Grid current

6 Conclusion

In this paper, a direct connection configuration of a supercapacitor string into a grid-tied PV generation system was proposed. The SC string is used to perform the MPPT of the PV modules. The voltage variation for MPPT is carried out by connecting or disconnecting the SC units in the SC string. The proposed configuration and its MPPT strategy have been verified through MATLAB/Simulink simulations. The proposed system is found cost-effective for commercial application. This study opens up a wider opportunity to do further studies regarding the enhancement of fault ride-through or power smoothing capabilities using the proposed direct connection of supercapacitors string scheme.

The authors currently are working on a real-time hardware implementation of the proposed scheme for a further verification that the scheme is also practically implementable adding a ramp-rate control capability to the proposed topology.

Acknowledgements

The authors would like to thank Dr. Md. Islam for providing real irradiance and temperature data and Dr. Rachid Errouissi for the suggestions in control of the grid-side inverter part.

References

[1] Trends in Photovoltaic Applications [Online]. Available: http://iea-pvps.org/

[2] D. Rekioua and E. Matagne, *Optimization of photovoltaic power systems: modelization, simulation and control*: Springer Science & Business Media, 2012.

[3] A. Labouret and M. Villoz, *Solar Photovoltaic Energy*: Institution of Engineering and Technology, 2010.

[4] F. Blaabjerg, C. Zhe, and S. B. Kjaer, "Power electronics as efficient interface in dispersed power generation systems," *IEEE Transactions on Power Electronics,* vol. 19, pp. 1184-1194, 2004.

[5] M. Liserre *, F. Blaabjerg, and A. Dell'Aquila, "Step-by-step design procedure for a grid-connected three-phase PWM voltage source converter," *International Journal of Electronics,* vol. 91, pp. 445-460, 2004/08/01 2004.

[6] P. Thounthong, V. Chunkag, P. Sethakul, S. Sikkabut, S. Pierfederici, and B. Davat, "Energy management of fuel cell/solar cell/supercapacitor hybrid power source," *Journal of Power Sources,* vol. 196, pp. 313-324, 1/1/ 2011.

[7] *BU-209: How does a Supercapacitor Work?* Available: http://batteryuniversity.com/learn/article/whats_the_role_of_the_supercapacitor

[8] N. Kakimoto, H. Satoh, S. Takayama, and K. Nakamura, "Ramp-Rate Control of Photovoltaic Generator With Electric Double-Layer Capacitor," *IEEE Transactions on Energy Conversion,* vol. 24, pp. 465-473, 2009.

[9] P. Barrade, S. Delalay, and A. Rufer, "Direct Connection of Supercapacitors to Photovoltaic Panels With On–Off Maximum Power Point Tracking," *IEEE Transactions on Sustainable Energy,* vol. 3, pp. 283-294, 2012.

[10] M. G. Villalva, J. R. Gazoli, and E. R. Filho, "Comprehensive Approach to Modeling and Simulation of Photovoltaic Arrays," *IEEE Transactions on Power Electronics,* vol. 24, pp. 1198-1208, 2009.

[11] G. M. S. Islam, A. Al-Durra, S. M. Muyeen, and J. Tamura, "Low voltage ride through capability enhancement of grid connected large scale photovoltaic system," in *IECON 2011 - 37th Annual Conference on IEEE Industrial Electronics Society*, 2011, pp. 884-889.

[12] M. A. Mahmud, H. R. Pota, and M. J. Hossain, "Dynamic Stability of Three-Phase Grid-Connected Photovoltaic System Using Zero Dynamic Design Approach," *IEEE Journal of Photovoltaics,* vol. 2, pp. 564-571, 2012.

[13] V. Kaura and V. Blasko, "Operation of a phase locked loop system under distorted utility conditions," *IEEE Transactions on Industry Applications,* vol. 33, pp. 58-63, 1997.

[14] F. Blaabjerg, R. Teodorescu, M. Liserre, and A. V. Timbus, "Overview of Control and Grid Synchronization for Distributed Power Generation Systems," *IEEE Transactions on Industrial Electronics,* vol. 53, pp. 1398-1409, 2006.

[15] S. M. Muyeen, H. M. Hasanien, and J. Tamura, "Reduction of frequency fluctuation for wind farm connected power systems by an adaptive artificial neural network controlled energy capacitor system," *IET Renewable Power Generation,* vol. 6, pp. 226-235, 2012.

[16] Maxwell Technologies - D Cell Series Ultracapacitor Documents [Online]. Available: http://www.maxwell.com/images/documents/bcseries_ds_1017105-4.pdf

[17] T. Esram and P. L. Chapman, "Comparison of Photovoltaic Array Maximum Power Point Tracking Techniques," *IEEE Transactions on Energy Conversion,* vol. 22, pp. 439-449, 2007.

[18] R. Takahashi, M. Nakatani, J. Tamura, S. M. Muyeen, M. Sugimasa, A. Komura*, et al.*, "Smoothing control of wind farm output fluctuation by new scheme with energy storage system," in *Power Electronics and Applications (EPE 2011), Proceedings of the 2011-14th European Conference on*, 2011, pp. 1-9.

[19] S. M. Muyeen, R. Takahashi, and J. Tamura, "Electrolyzer switching strategy for hydrogen generation from variable speed wind generator," *Electric Power Systems Research,* vol. 81, pp. 1171-1179, 5// 2011.